Int. J. Solids Structures Vol. 22, No. 9, pp. 1007–1017, 1986
Printed in Great Britain

0020–7683/86 $3.00 + .00
Pergamon Journals Ltd

ELASTIC-PLASTIC BUCKLING DESIGN OF CYLINDRICAL SHELLS SUBJECT TO COMBINED AXIAL COMPRESSION AND PRESSURE LOADING

C. P. ELLINAS
J. P. Kenny & Partners Ltd.,† High Holborn, London, U.K.

and

J. G. A. CROLL
Civil Engineering Department, University College, London, U.K.

(*Received* 6 *March* 1984; *in revised form* 11 *July* 1985)

Abstract—A recently developed procedure for predicting the elastoplastic axisymmetric collapse of cylinders subjected to combinations of axial compression and pressure loading is described. This allows the modelling of radial pressure induced deformations, boundary effects and initial geometric imperfections in terms of an equivalent imperfection in a "column type" bifurcation analysis. Together with the incorporation of a more rational means of specifying initial geometric tolerances, it is used to develop compact design-orientated procedures for predicting safe design loads for this form of elastoplastic collapse of cylinders.

INTRODUCTION

Local inter-ring buckling of ring stiffened cylinders may take one of two distinct forms. Where the subshell cylinders are very slender, elastic effects tend to dominate, and buckling is usually triggered by modes having circumferentially wavy forms. For more stocky subshell cylinders, it is common for material plasticity to occur at an early stage of the loading process and for buckling to be initiated near the boundaries in modes having axisymmetric forms. Present concern is with the latter axisymmetric form of buckling.

A recently developed procedure for predicting the elastic-plastic axisymmetric collapse of cylinders subjected to arbitrary combinations of axial, and radial pressure loading[2] is briefly summarized. This procedure is based upon two key notions. First, the analysis makes use of a "perfect cylinder" concept for which an external radial pressure is introduced that is just sufficient to overcome the Poisson bulging, otherwise caused by axial loading. In this way the nonlinear elastic behaviour can be modelled in terms of a classical axisymmetric bifurcation from the perfectly cylindrical shape. Arbitrary radial pressure, Poisson bulging, the effects of boundary deformations caused by ring flexural and torsional flexibilities, as well as any initial imperfections in the shell's geometry, can all then be modelled in terms of an equivalent imperfection for this "column-type" bifurcation. Based upon this convenient and exact modelling of the elastic nonlinearities, the second notion is that of using the elastic stress and moment resultants to determine the loads producing first surface yield and first full section plasticity in the shell. With this full plasticity occurring over an entire circumference of the cylinder, its attainment is shown to provide an accurate indication of the total collapse of the cylinder.

Quite apart from the analytic simplicity it offers, it is demonstrated how this modelling provides a compact and practically attractive means for presenting axisymmetric buckling loads for combined axial and pressure loading. It also allows the incorporation of what we believe to be more rational means of specifying initial geometric tolerance limits.

For analytical convenience, the end conditions of the cylinders are taken to be those of the classical simple support. The treatment of other end conditions could follow the same general procedure.

† Formerly, Civil Engineering Department, University College, London, U.K.

ELASTIC BEHAVIOUR

The axisymmetric elastic response of cylinders under axial and pressure loading is known to display an at times highly nonlinear character. Various numerical procedures have been used to predict this nonlinearity[5, 7, 8], but each requires the aid of considerable computation facilities. The following alternative could easily be incorporated into the small scale computing facilities available in most design offices.

An isotropic cylinder of radius, r, length, ℓ, and thickness, t, is subjected to an axial load P and an external radial pressure $p(=\mu P/2\pi r^2)$ such that the membrane fundamental stresses are

$$\sigma_x^F = -P/2\pi rt = -\sigma, \qquad (1)$$
$$\sigma_\theta^F = -p(r/t) = -\mu\sigma.$$

With this uniform fundamental stress state involving zero circumferential strain, ε_θ^L, the shell would retain its original cylindrical shape.

From such a purely membrane fundamental state, and it may be observed that the membrane state of eqn (1) is the exact solution, there exists an infinite set of critical stresses σ_{cj}.

$$\frac{\sigma_{cj}}{\sigma_{cl}} = \frac{1}{2}\left[\left(\frac{j}{j_{cl}}\right)^2 + \left(\frac{j_{cl}}{j}\right)^2\right] \qquad (2)$$

representing bifurcations into axisymmetric critical modes

$$w = w_j \sin(j\pi x/\ell) \qquad (3)$$

having j axial half-waves. The classical critical stress $\sigma_{cl} = Et/\{r[3(1-\mu^2)]^{1/2}\}$ is the minimum of this set of critical stresses for a cylinder long enough that the classical critical wave number $j_{cl} = S/3^{1/4}$ would provide an integer division of the shell's length. The composite geometric parameter S is related to the more familiar Batdorf parameter Z through $S = (6Z)^{1/2}/\pi$, where $Z = \ell^2(1-\mu^2)^{1/2}/(rt)$.

Provided there is no interaction with nonaxisymmetric modes, that is no bifurcation from the axisymmetric into a circumferentially periodic mode, the bifurcation behaviour into each of the constituent modes w_j is essentially neutral. This means that at an axial compressive stress, σ, the modal displacements would take the same form as those of a column, namely

$$(w_j - \bar{w}_j) = [\sigma/(\sigma_{cj} - \sigma)]\bar{w}_j, \qquad (4)$$

in which $\bar{w}_j$ are the modal imperfections and w_j the total modal displacements. The complete displacement is then given by

$$(w - \bar{w}) = \sum_{j=1,3,5,} \left(\frac{\sigma}{\sigma_{cj} - \sigma}\right)\bar{w}_j, \qquad (5)$$

where it is assumed that the buckled form is symmetric about the midlength of the cylinder.

Modal imperfections $\bar{w}_j$ are made up of two parts: initial geometric imperfections w_j^0 and equivalent loading imperfections w_j^L.

Initial geometric imperfections

These are dominantly determined by the particular form of fabrication process adopted. Subsequent damage can contribute to axisymmetric imperfections but has a more pronounced effect on the nonaxisymmetric imperfections. Fabrication axisymmetric imperfections will generally result from any lack of fit and shrinkage associated with welding

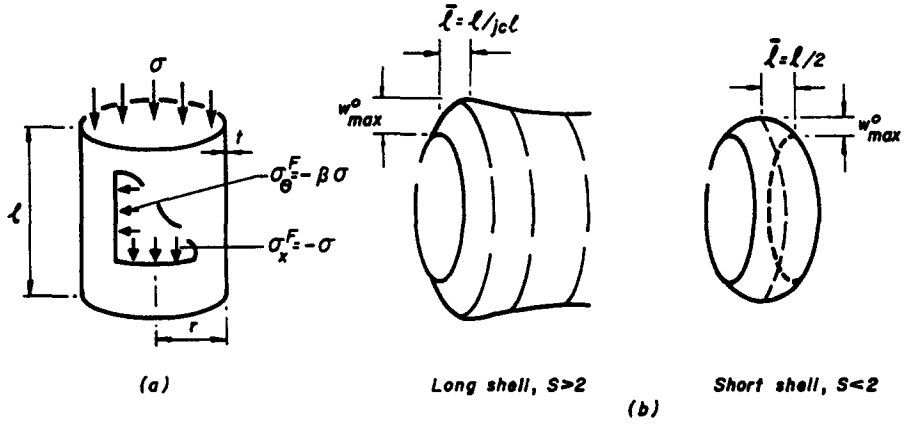

Fig. 1 (a) Notation and convention, and (b) nature of axisymmetric imperfections for shells of varying geometries.

at circumferential seams and at connections to rings or frames. They often take the form shown exaggerated in Fig. 1(b). Provided the shell is long enough an edge bending shear q_0 would give rise to localized boundary layer distortions that can be shown to have distributions similar to those in Fig. 2. In plotting the profiles of Fig. 2 the edge shear q_0 was maintained constant. What Fig. 2 also shows is that beyond a certain critical value of the parameter S the actual shape of the edge disturbance remains invariant. Furthermore, the location of the maximum distortion can be seen to occur at a distance $\bar{\ell}$ from either end, where $\bar{\ell}$ corresponds with the critical half-wave length given by

$$\bar{\ell} = \min\begin{cases} \ell/2, & \text{when } j_{cl} \leqslant 2, \\ \ell/j_{cl}, & \text{when } j_{cl} > 2. \end{cases} \tag{6}$$

The magnitude of this maximum distortion may be expressed as

$$w^0_{max}/t = f(S)\,(\bar{w}^0_{max}/t), \tag{7}$$

where $\bar{w}^0_{max}$ would represent the maxima produced when $S \to \infty$, and $f(S)$ is the function giving the variation of the maxima corresponding to a constant value of the end shear q_0. Its distribution is shown in Fig. 3, where it is also shown by the broken line that a reasonable

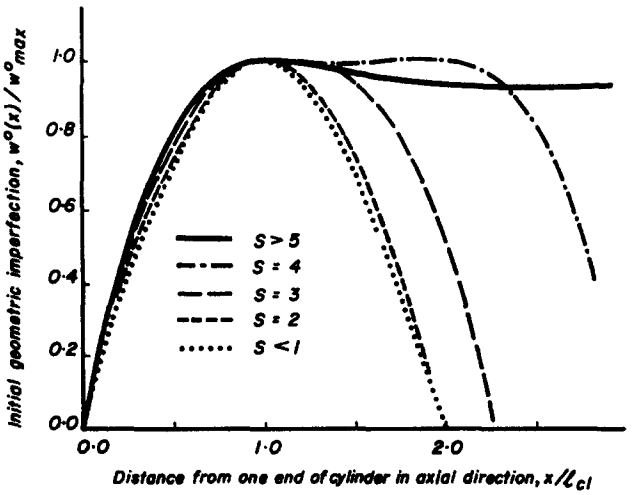

Fig. 2. Variation in initial geometric imperfection, $w^0(x)$, with shell geometric parameter S.

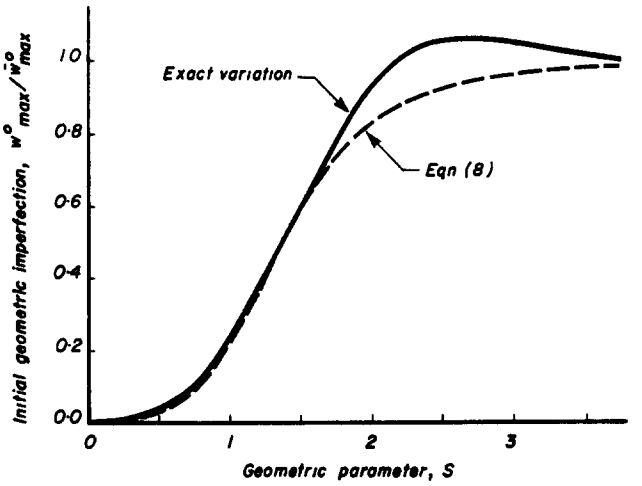

Fig. 3. Variation in maximum tolerance, w^0_{max}, with shell geometric parameter S

approximation of this exact variation of the maxima is

$$\frac{w^0_{max}}{t} = \frac{1}{[1+(1.375/S)^4]} \frac{\bar{w}^0_{max}}{t}. \tag{8}$$

Having decided upon the tolerance $\bar{w}^0_{max}/t$ to be adopted for a long cylinder, eqn (8) then provides the scaling factor to be applied to allow in a rational way for the effects of the shell length. It is this procedure for consistently relating tolerances to some specified fabrication process that is adopted in the numerical examples that follow.

It has been observed that the out-of-straightness imperfections, $\bar{w}^0_{max}$, in fabricated cylinders are functions of $(rt)^{1/2}$. For this reason most Design Codes have adopted tolerance specifications in the form

$$\bar{w}^0_{max} = k(rt)^{1/2}, \tag{9}$$

with DnV[3] using $k = 1/30$, while DASt Ri O13[4] and ECCS[6] adopt $k = 1/25$. Our present description of fabrication imperfections provides a useful theoretical explanation for such an empirically based tolerance specification.

Typical circumferential welds are shown in Fig. 4. The area of the weld is proportional to (t^2), so that the hoop force induced by weld shrinkage would take the form $N_w = b_1\sigma_y t^2$, where the constant b_1 would be governed by the shape and the actual process adopted for the weld, and σ_y is the yield stress of the material. Radial equilibrium then demands that

$$q_w = b_2\sigma_y(t^2/r), \tag{10}$$

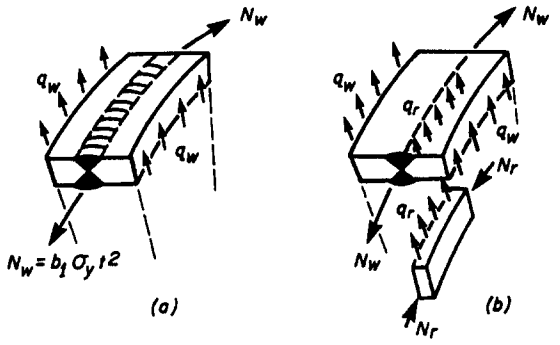

Fig. 4. Nature of weld shear q_w induced by residual stresses arising from circumferential welding.

where $b_2 = \frac{1}{2}b_1$ for the case of the simple seam weld in Fig. 4(a), but would depend upon the proportion of the shrinkage absorbed by the ring stiffener in Fig. 4(b). For a long cylinder, the edge shear may be written in the form

$$q_0 = b_3 E(t/r)^{3/2}\bar{w}^0_{\max}, \tag{11}$$

where b_3 is constant for long shells having $S \geqslant 5$ ($b_3 = 0.336$ for the present simply supported boundary). Equating eqns (10) and (11), it follows that provided the shell is sufficiently long, the maximum distortion would be given by

$$\bar{w}^0_{\max} = b_4(\sigma_y/E)(rt)^{1/2}, \tag{12}$$

which is of a similar form to eqn (9) adopted in most Codes. In addition, the gauge length ℓ_g over which such an out-of-straightness would occur appears from eqn (6) and Fig. 5 to be given by

$$\ell_g = 2\bar{\ell} = \min\begin{cases}\ell, \\ 2\ell/j_{cl} = 3.46(rt)^{1/2}.\end{cases} \tag{13}$$

Again, this compares closely with the gauge lengths adopted in most Design Codes[3, 4, 6], where the gauge length is specified as the lesser of $4(rt)^{1/2}$ and usually the ring spacing ℓ.

The above outlined method provides a means of specifying tolerances which is at once consistent with present design practice and empirical observation. Equation (8) would appear to provide a more rational and consistent way of allowing for the effects of length changes than that sometimes adopted in existing practice.

Loading imperfections

These arise whenever an arbitrary external pressure produces a hoop compressive stress of $\beta\sigma$, such that $\beta \neq \mu$. In this case a proportionate loading system will produce modal imperfections which are given by (details of this derivation are given in [2])

$$\frac{w^L}{t} = \frac{4(\beta-\mu)(r/t)}{\pi j(1+j^2)}\frac{\sigma_{cl}}{E} = \frac{2(\beta-\mu)}{[3(1-\mu^2)]^{1/2}jJ\pi}, \tag{14}$$

where $J = (j/j_{cl})^2$. Similar expressions could be obtained for end boundary conditions other than the present simple supports.

Elastic nonlinearity

This is now given by eqn (5) provided that the total modal imperfection $\bar{w}_j$ is represented as

$$\frac{\bar{w}_j}{t} = \left(\frac{w^L_j}{t} + \frac{w^0_j}{t}\right). \tag{15}$$

To demonstrate the forms of the nonlinear solutions obtained from eqn (5), using the

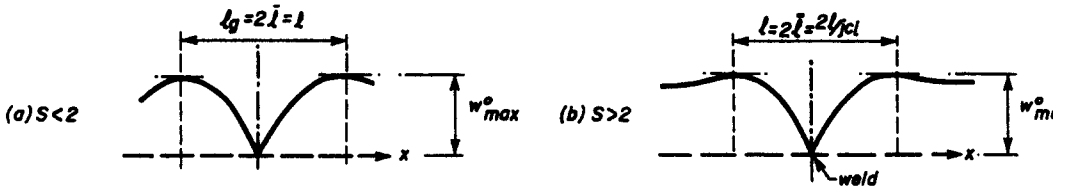

Fig. 5. Form of shell distortion caused by residual stresses from circumferential welding.

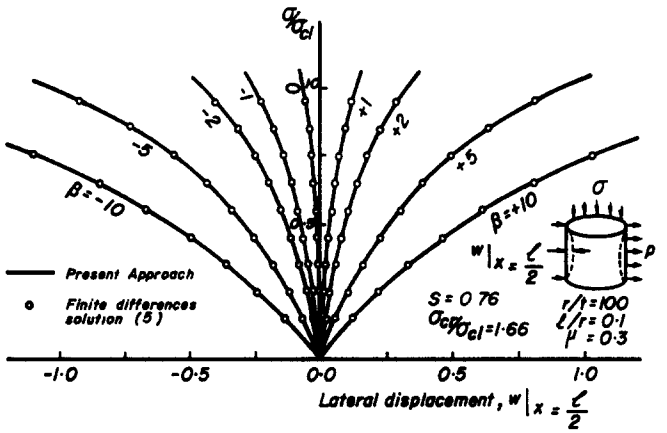

Fig. 6(a). Nonlinear elastic behaviour as a function of parameter β, for a shell with $S = 0.76$.

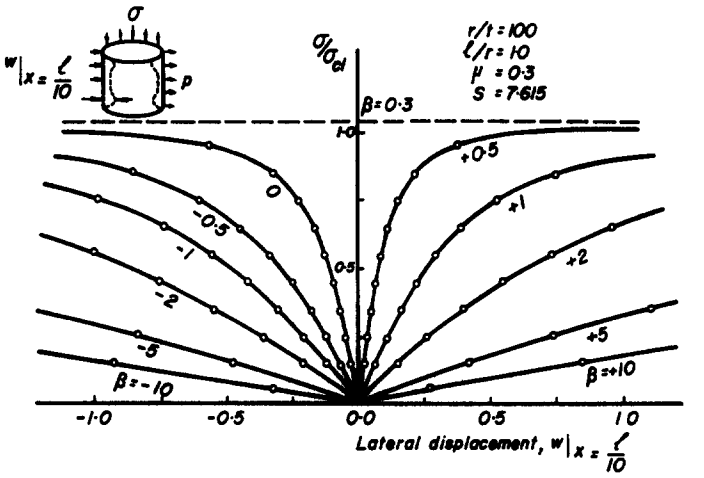

Fig 6(b). Nonlinear elastic behaviour as a function of parameter β, for a shell with $S = 7.615$.

equivalent imperfections in eqn (15), Fig. 6 shows the stress-displacement plots for two illustrative examples. In Fig. 6(a) a typical short shell is depicted for which $j_{cl} < 1$, while Fig. 6(b) shows the case of a long shell having $j_{cl} \gg 1$. It can be seen that the present analytically simple solution is in very good agreement with a solution based upon a finite difference modelling of the full nonlinear equations governing the axisymmetric behaviour of cylindrical shells[5].

It is this analytically simple description of axisymmetric elastic nonlinearity, contained in eqns (5) and (15), that is incorporated into the following criterion for assessing incipient elastic-plastic collapse.

ELASTIC-PLASTIC BEHAVIOUR

Making use of a similar procedure to that recently developed for nonsymmetric elastic-plastic collapse of cylinders[1], the above symmetric nonlinear elastic solution is used to provide a statically admissible force field for determining first surface yield and first full section plasticity (denoted σ_{Fy} and σ_{Fp}, respectively). First surface yield, based upon this approach, would be exact, while the neglect of possible redistribution in stress and moment resultants caused by plastic nonlinearities means that the present full section plasticity stress provides only an approximation of the actual collapse stress σ_b.

First surface yield

It is a fairly straight-forward procedure to superimpose the buckling stresses accompanying the growth of modal displacements w_j[2] on the fundamental membrane stresses of eqn (1) to determine the total stresses. On the basis of a von Mises deformation energy yield criterion

$$\sigma_x^2 - \sigma_x\sigma_\theta + \sigma_\theta^2 < \sigma_y^2 \tag{16}$$

first surface yield is found to occur very close to the circumference at a distance $x = \ell/(2j_{(i)})$ from either end of the shell. Figure 7 shows the first yield stresses obtained on the present basis for the two shells considered in Fig. 6. For each shell two cases are given. In the first there is no initial imperfection, so that $w^0 = 0$. For this case a loading corresponding with $\beta = \mu$ would also involve no loading imperfections w^L, so that the shell would remain cylindrical for all stresses σ. Without bending effects, the fundamental stress state of eqn (1) would from eqn (16) reach yield when

$$\sigma_{0sq} = \sigma_y/(1-\mu+\mu^2)^{1/2} = 1.15\sigma_y, \tag{17}$$

which explains why in Fig. 7 $\sigma_{Fy} = \sigma_{Fp} = 1.15\sigma_y$ when $\beta = \mu$. The second example given for each shell is based upon a nominal tolerance of $\bar{w}^0 = (rt)^{1/2}/30$, as specified by DnV[3]. These

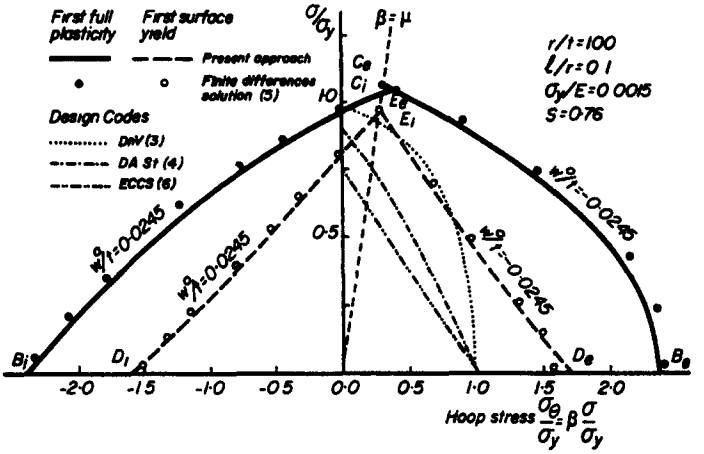

Fig. 7(a) Elastoplastic interactions between axial and hoop stresses for a shell with $S = 0.76$.

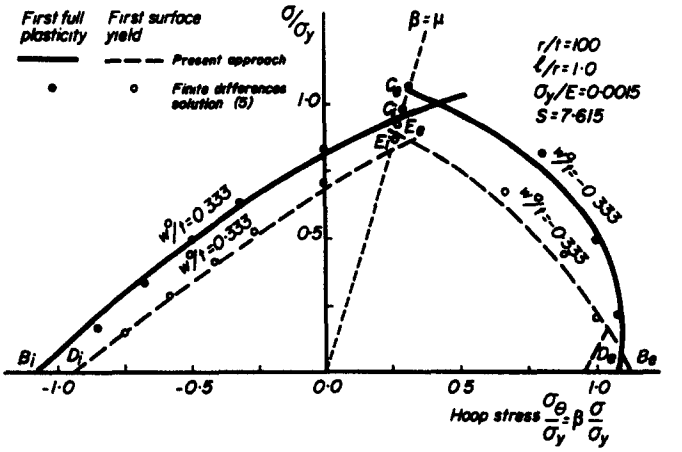

Fig. 7(b). Elastoplastic interactions between axial and hoop stresses for a shell with $S = 7.615$.

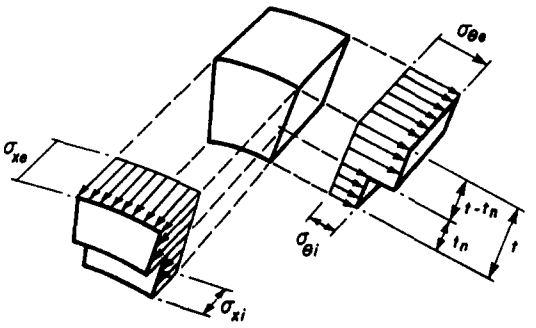

Fig. 8 Stress block on circumference attaining fully plastic state.

are then scaled according to eqn (8) to account for the length effect and give the actual maximum geometric imperfections listed. First yield under pure radial pressure, that is $\sigma_x = 0$, can be seen to be independent of geometric imperfections.

In obtaining the interaction diagrams of Fig. 7 it has been assumed that the shell has an equal probability of developing inward and outward initial geometric imperfections. In practice this is unlikely to be the case. Fabrication distortions are most likely to result in outward imperfections that have larger magnitudes than inward imperfections. This may mean that the lines E_eD_e, which are based upon inward imperfections of the same magnitudes as the outward imperfections of E_iD_i, are unnecessarily pessimistic.

First full section plasticity

A simple analytical solution to the first full section plasticity state has been described in [2]. This depends upon finding where the nonlinear elastic stress and moment resultants reach the full plastic state shown in Fig. 8. The only approximation involved in such a full section plasticity state is that of assuming just one stress discontinuity at t_n. However, the results compared in Fig. 7 with those obtained on the basis of an Ilyushin full plasticity yield criterion[5], suggest that this approximation is of little consequence.

Before considering how interaction diagrams like those in Fig. 7 could be produced for practical design purposes, it is worth drawing-out some of the important features displayed in such interactions. For $\beta = \pm\infty$ (that is pure radial pressure) the first surface yield σ_{Fy} and first full plasticity σ_{Fp} stresses are independent of initial geometric imperfections w^0. For this loading case, collapse is entirely the result of what we have described here as equivalent load imperfections. Moreover, collapse depends only on the linear elastic response. Limit states under these circumstances were described by Hodge[9]. For $\beta = \mu$,

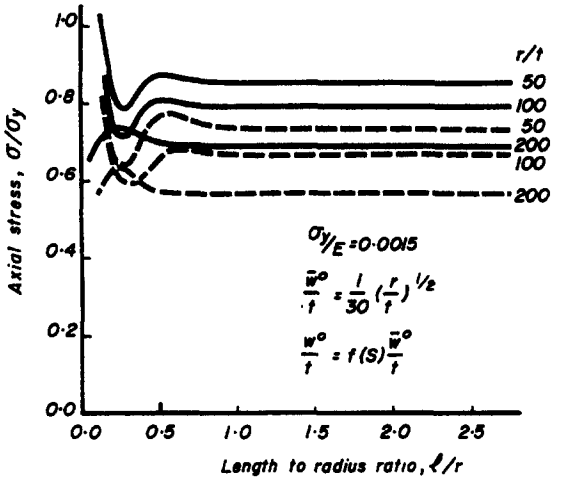

Fig. 9. First yield (- - -) and first full plasticity (—) for axially loaded imperfect cylinders.

as already observed, the first yield and full plasticity stresses are independent of equivalent load imperfections w^L. In this case the reductions in load carrying capacity are entirely the result of initial geometric imperfections w^0. These features will be made use of in the next section.

One case of loading that has importance in its own right is that of pure axial loading, $\beta = 0$. Figure 9 shows the reductions in σ_{Fy} and σ_{Fp} over a wide range of geometric parameters for shells containing outward imperfections whose magnitudes are based on those specified by DnV[3] but modified according to eqn (8). What Fig. 9 shows is that for a fixed r/t and beyond a certain length there is no further change in collapse load as ℓ/r increases. What is not shown in Fig. 9 is that these curves would be almost unchanged by using steel having yield stresses over the range $0.001 < \sigma_y/E < 0.0025$ of practical mild steels.

A DESIGN APPROACH

It may be observed in Fig. 7 that both first yield lines E_iD_i and E_eD_e (the subscripts indicate that first yield occurs on the internal and external faces, respectively), as well as the first full plasticity lines C_iB_i and C_eB_e are very nearly straight lines. The convexity that occurs in say the perfect collapse lines AB_i and AB_e is very much reduced by the presence of geometric imperfections. This suggests that if the various points B, D and C, E can be defined, a simple linear interpolation could be used to construct slightly conservative interaction diagrams for both σ_{Fy} and σ_{Fp}.

Taking first the reductions occurring for the load case $\beta = \mu$. For this proportionate loading system, there would be no loading imperfections w^L. Reductions in buckling loads from the idealized squash pressure $\sigma_{\theta sq} = 1.15\sigma_y$ are entirely due to initial geometric imperfections. The degree of reduction can be shown[2] to depend upon just two parameters; the ratio of the classical elastic critical stress to material yield stress, σ_{cl}/σ_y, and the magnitude of the prescribed initial imperfection or tolerance limit, w^0/t. However, in the present context where the initial imperfections are taken in the form specified by DnV[3], but modified to allow for the effects of shell length, all shell geometric and material parameters influence the knock-down factors, particularly for short and/or long shells. When the shell is long enough, $S > 5$, the imperfection shape and magnitude become independent of ℓ/r. This is reflected in the invariance of σ_{Fy} and σ_{Fp} when $\ell/r \gtrsim 5(t/r)^{1/2}$, shown in Fig. 10. It may be observed that for a given level of imperfection an outward initial imperfection, Fig. 10(a),

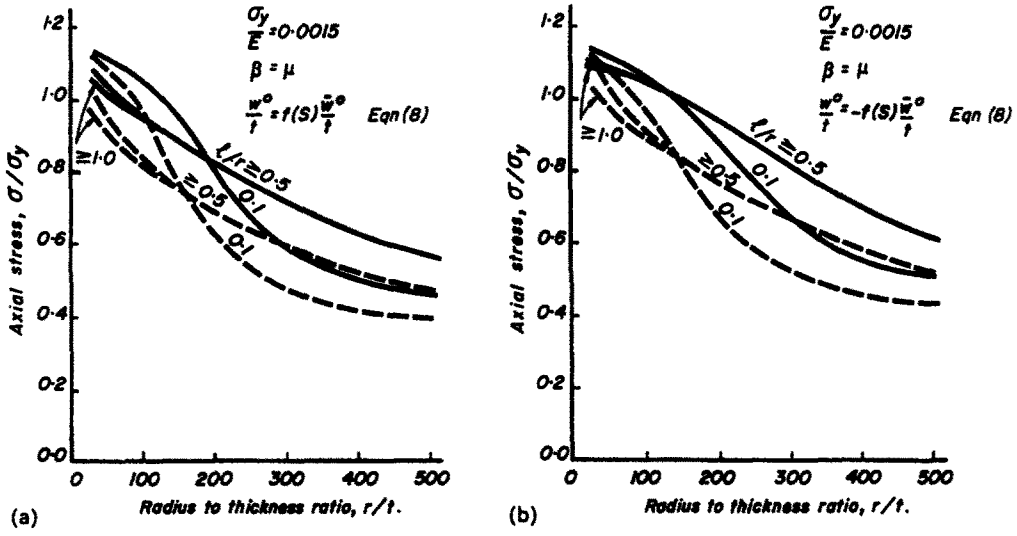

Fig. 10. First yield (- - -) and first full plasticity (—) for imperfect cylinders under combined loading for which, $\beta = \mu$. (a) Inward imperfections, and (b) outward imperfections.

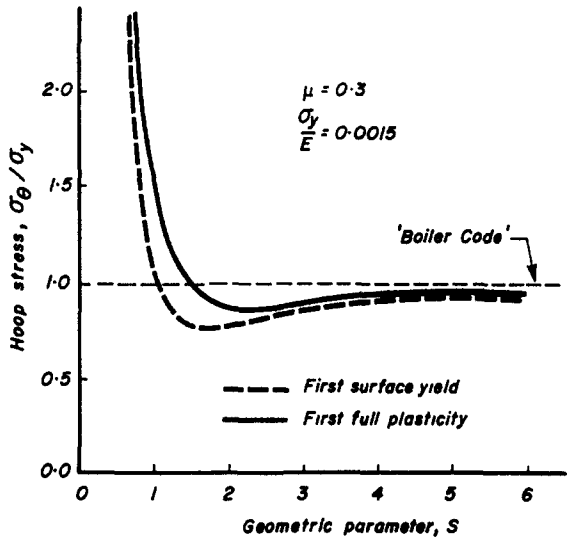

Fig. 11. First yield and first full plasticity for shells under pure radial pressure loading

produces a slightly higher reduction than an inward one, Fig. 10(b). If the possibility of using smaller tolerance limits on inward imperfections than on outward imperfections were incorporated, the separations of the pairs of points (E_i, E_e) and (C_i, C_e) would be even greater than those shown on Fig. 7.

For the particular case of pure radial pressure loading (for which $\sigma_x = 0$ and $\beta \to \infty$) the first yield and first full plasticity states are independent of initial imperfections w^0. The critical locations occur in the vicinity of the boundary layer, and the collapse loads may be conveniently summarized as in Fig. 11. In this case the effects coming from shell geometry can be encapsulated into the single composite parameter S. Practical variations in material yield stress have virtually no effect on the first yield and first full plasticity stresses shown in Fig. 11.

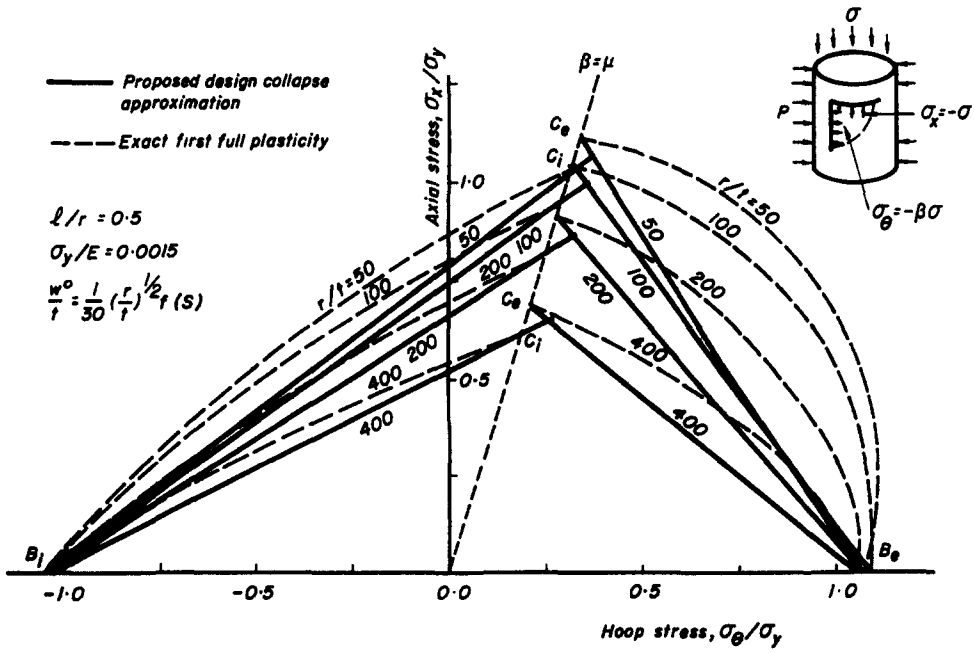

Fig. 12. Comparisons of simplified design curves for plastic collapse (based upon Figs. 10 and 11) and the exact interaction curves. Tolerances w^0 according to DnV[3], but modified by eqn (8) to allow for consistent fabrication process.

Based upon the nominal imperfection $\bar{w}^0/t = (r/t)^{1/2}/30$, and modified according to eqn (8), a sample set of simple design curves taken from the buckling loads summarized in Figs. 10 and 11, are shown in Fig. 12. Shown also are the exact curves for each r/t ratio. This approximate procedure for producing design curves provides a much closer representation of the axisymmetric buckling collapse than would a linear interpolation between the points on the σ_x/σ_y and σ_θ/σ_y axes, corresponding to $\beta = 0$ and $\beta = \pm\infty$. Moreover, the recommended use of $\beta = \mu$ and $\beta = \pm\infty$ allows proper incorporation of differential tolerance limits on inward and outward axisymmetric bulging. Where existing Design Codes provide interactive buckling curves they do not distinguish axisymmetric from nonaxisymmetric collapse. As a result the linear and sometimes nonlinear interpolations employed are based upon the $\beta = 0$ and $\beta = \pm\infty$ load cases, which as shown by the incorporation of the DnV[3] and ECCS[6] curves in Fig. 7(a) can be unreasonably conservative.

CONCLUSIONS

The simple analytic procedure summarized has been shown to provide a convenient and accurate means for estimating the axisymmetric collapse loads of cylinders loaded under arbitrary combinations of axial and pressure loading. The incorporation of tolerance limits on initial imperfections, based on physical reasoning that has been shown to be consistent with empirical observation and current design practice, has led to the development of a rational approach to the derivation of load-interaction curves, that allows for the influence of length effects on imperfection levels.

Two important features of these interaction curves have been identified that make the construction of any required design curves simple and accurate. The first is based on the notion of a "perfect cylinder" where reductions in load carrying capacity are entirely due to geometric imperfections, and the second is based on the pure radial pressure loading case which has been shown to be independent of geometric imperfections. These two easily identifiable stress states and their corresponding estimates of collapse can be used to construct any desired design interaction curves for the axisymmetric buckling collapse of axial and pressure loaded cylinders.

Acknowledgements—The authors are indebted to the Science and Engineering Research Council of Great Britain for their support through a grant made available to the London Centre for Marine Technology.

REFERENCES

1. J. G. A. Croll, Elasto-plastic buckling of pressure and axial loaded cylinders. *Proc. Instn Civil Engineers* **73**, 633–652 (1982).
2. J. G. A. Croll, Axisymmetric elastic-plastic buckling of axial and pressure loaded cylinders. *Proc. Instn Mech. Engineers* **198C**, 243–259 (1984).
3. Det norske Veritas (DnV), "Rules for the Design, Construction and Inspection of Offshore Structures—Appendix C: Steel Structures." Norway, 1979.
4. Deutscher Ausschuss fur Stahlbau (DASt), "Beulsicherheitsnachweise fur Schalen." DASt Richtlinie 013, Cologne, Germany, 1980.
5. C. P. Ellinas, Axisymmetric Buckling of Axial and Pressure Loaded Ring Stiffened Cylinders. SS Report, London Centre for Marine Technology, 1982.
6. European Convention for Constructional Steelwork (ECCS), "European Recommendations for Steel Construction–Section 4.6: Buckling of Shells." The Construction Press, London, 1981.
7. J. E. Harding, Ring-stiffened cylinders under axial and external pressure loading. *Proc. Instn Civil Engineers* **71**, 863–878 (1981).
8. A. Andronicou and A. C. Walker, Buckling of ring stiffened shells subject to pressure and axial loading, to be published.
9. P. G. Hodge, *Limit Analysis of Rotationally Symmetric Plates and Shells*. Prentice Hall, Englewood Cliffs, New Jersey.